ARTICLE

Application of Laser Dispersion Method in Apparatus Combining H Atom Rydberg Tagging Time-of-Flight Technique with Vacuum Ultraviolet Free Electron Laser†

Yao Chang[a,b‡], Zhi-gang He[b‡], Zi-jie Luo[b,c‡], Jia-mi Zhou[b], Zhi-guo Zhang[d*], Zhi-chao Chen[b], Jia-yue Yang[b], Yong Yu[b], Qin-ming Li[b], Li Che[c], Guo-rong Wu[b], Xing-an Wang[a], Xue-ming Yang[b], Kai-jun Yuan[b*]

a. Department of Chemical Physics, School of Chemistry and Materials Science, University of Science and Technology of China, Hefei 230026, China
b. State Key Laboratory of Molecular Reaction Dynamics, Dalian Institute of Chemical Physics, Chinese Academy of Sciences, Dalian 116023, China
c. Department of Physics, School of Science, Dalian Maritime University, Dalian 116026, China
d. Key Laboratory of Functional Materials and Devices for Informatics of Anhui Higher Education Institutions and School of Physics and Electronic Engineering, Fuyang Normal University, Fuyang 236041, China

(Dated: Received on January 13, 2020; Accepted on February 11, 2020)

Photodissociation of H_2S in the VUV region plays an important role in the atmospheric chemistry and interstellar chemistry. To date, however, few studies have been focused on this topic. In this article, we have described a laser dispersion method applied in the apparatus combining the high-n H atom Rydberg tagging time-of-flight technique with the vacuum ultraviolet free electron laser (VUV FEL). The Lyman-α laser beam (121.6 nm) used in the H-atom detection was generated by the difference frequency four-wave mixing schemes in a Kr/Ar gas cell. After passing through an off-axis biconvex LiF lens, the 121.6 nm beam was dispersed from the 212.6 nm and 845 nm beams due to the different deflection angles experienced by these laser beams at the surfaces of the biconvex lens. This method can eliminate the background signal from the 212.6 nm photolysis. Combined with the VUV FEL, photodissociation of H_2S at 122.95 nm was studied successfully. The TOF spectrum was measured and the derived total kinetic energy release spectrum was displayed. The results suggest that the experimental setup is a powerful tool for investigating photodissociation dynamics of molecules in the VUV region which involves the H-atom elimination processes.

Key words: Photodissociation, Vacuum ultraviolet, Free electron laser

I. INTRODUCTION

As an engine of atmospheric and interstellar chemical processes, molecular photodissociation is of great importance for atmospheric and interstellar science [1, 2]. Photodissociation induced by the absorption of single photon permits the detailed study of molecular dynamics such as the breaking of bonds, internal energy transfer and radiationless transitions. Over the last decades, the availability of powerful lasers operated over a wide frequency range [3–6] has stimulated rapid development of new experimental techniques [7–10] which make it possible to study photodissociation processes in unprecedented detail. At the same time, theorists have developed powerful methods to treat these fundamental processes, at least for small polyatomic molecules, in an essentially exact quantum mechanical way. The confluence of theory and experiment has greatly advanced understanding of molecular motion in excited electronic states.

In the recent decades, due to the development of the intense ultraviolet (UV) light sources using nonlinear crystals such as KDP and BBO, great advances have been obtained in molecular photodissociation in the UV region (200−400 nm). However, the vacuum ultraviolet (VUV) photodissociation studies are only focused on the wavelengths of 193 nm and 157.6 nm, which are generated by the commercial excimer lasers. Later, the development of Four-Wave Mixing (FWM) techniques provided an opportunity to study the molecular photodissociation in a wide VUV region. Noble gases (Xe [6], Kr [4, 11], Ar [12], and Ne [13]) are frequently employed as the nonlinear media, as they have appropriate

†Part of the special topic on "The 35th International Symposium on Free Radicals (ISFR 2019)".
‡These authors contributed to this work equally.
*Authors to whom correspondence should be addressed. E-mail: zhgzhang@mail.ustc.edu.cn, kjyuan@dicp.ac.cn

energy-level structures and are more convenient to use than mercury (Hg) vapor [14–16]. Meanwhile, VUV generation by resonant third-order difference frequency FWM ($\omega_{\rm VUV}$=$2\omega_{\rm R}$−$\omega_{\rm T}$) in Kr has been investigated with flying colors. The frequency $\omega_{\rm R}$ (212.6 nm) is resonant with the Kr two-photon transition 4p−5p [1/2, 0]. By tuning $\omega_{\rm T}$ in the range of 220−860 nm, it is possible to generate $\omega_{\rm VUV}$ in the wavelength range 121−190 nm [17]. As to the VUV region below 120 nm, resonance-enhanced sum-frequency FWM ($\omega_{\rm VUV}$=$2\omega_{\rm R}$+$\omega_{\rm T}$) needs to be employed [18, 19]. For the specific Lyman-α wavelength (121.6 nm), by adding three times volume Ar into Kr, the phase matching makes it possible to use higher gas pressures and significantly enhances conversion efficiency, facilitating the production of $\sim10^{12}$ photons/pulse [17]. However, such phase matching is not universal, which means that the light intensities of VUV beams at most wavelengths produced by FWM are relatively weak. This causes some difficulty for investigating the VUV molecular photodissociation in which the photoabsorption cross section of molecules are quite small. Another intense VUV beam source is a third generation synchrotron, which provides $\sim10^{16}$ photons/s with an energy resolution, $\Delta E/E$, of ∼1% [20]. The quasi-continuous nature of synchrotron radiation generally prohibits some applications, such as photodissociation, in which the high peak VUV powers are required. Recently, the development of VUV free electron laser (FEL) at the Dalian Coherent Light Source (DCLS) has provided an extremely powerful VUV source, the pulsed energy of which is many orders of magnitude higher than other VUV sources used thus far. Photodissociation dynamics of H_2O at 111.5 nm [21] and 115.2 nm [22] have been investigated successfully by using this VUV source combined with the H atom Rydberg tagging time of flight technique (HRTOF).

The HRTOF technique, providing the extremely high translational energy resolution, has been widely applied in the study of the H-elimination process in molecular photodissociation [23–25] and chemical reactions [26, 27]. The key point in the HRTOF technique is the efficient excitation of the H atom, which involves absorbing one Lyman-α photon (121.6 nm) to excite the H atom from n=1 to n=2 level. The Lyman-α photon was usually generated by difference FWM schemes of 212.6 nm and 845 nm in a Kr/Ar mixing gas cell [17]. However, for some molecules, like H_2S [28] and NH_3 [29, 30] which have strong absorption cross sections at 212.6 nm, the background signals from 212.6 nm photolysis are extremely large. For some other molecules, like CH_4 [31] and C_2H_6, though they have very weak absorption cross sections at 212.6 nm, their primary dissociation products [32, 33] can be photodissociated by absorbing one 212.6 nm photon immediately. Thus, photodissociation dynamics of such molecules in the VUV region are quite difficult due to the 212.6 nm signal contamination. In this work, we designed a laser dispersion scheme [34, 35] applied in our new apparatus which has combined the HRTOF technique with the VUV FEL laser. Photodissociation dynamics of H_2S molecule in the VUV region were investigated by using this setup successfully, and the preliminary result at 122.95 nm photolysis has been presented here.

II. METHODOLOGY

The VUV FEL laser [8] and HRTOF technique [7, 36] have been described in detail previously, here is a brief description. The HRTOF technique used here was developed in the early 1990s by Welge *et al.* [36]. The central scheme of this technique is the sequential two-step excitation of the H atom. The first step involves the resonant excitation of the H atom from the n=1 to n=2 state at 121.6 nm. The second step concerns the UV laser excitation (365 nm) of the H atom from the n=2 state to a high-n (n=30−80) Rydberg state, lying slightly below the ionization threshold. Any charged species can be extracted away from the TOF axis by adding a weak electric field (∼30 V/cm) in the detection region. The neutral Rydberg H atoms flied a certain distance (∼280 mm) before reaching a Z-stack micro-channel plate (MCP) detector (FIG. 1) with a fine metal grid in the front. After passing through the grid, the Rydberg atoms were field-ionized immediately by the electric field (∼2000 V/cm) applied between the front plate of the Z-stack MCP detector [24] and the grounded fine metal grid. The signal detected by the MCP was then amplified by a fast pre-amplifier (ORTECVT120) and counted by a multichannel scaler (P7888).

The horizontal cutaway view of the experimental apparatus is shown in FIG. 2. The main vacuum chamber is a large stainless steel cube, evacuated by a 2000 L/s turbo-molecular pump (BOC EDWARDS STP-A2203C) and a 1600 L/s turbo-molecular pump (BOC EDWARDS STP-A1603C) backed by a pump station (Hicube 80 Eco, 35 L/s). The source chamber is separated from the main chamber by a stainless steel cover, which is pumped by another 2000 L/s turbo-molecular pump backed by the same pump station used in the main chamber. The pressure of the main chamber and the source chamber is typically 10^{-8} and 10^{-9} torr respectively (10^{-7} and 10^{-5} torr during the molecular beam operation). Meanwhile, for the purpose of decreasing the H atom background in the chamber, a cryo-pump (OXFORD, 350A) is employed in the main chamber.

FIG. 2 also displays the arrangement of the laser systems for generating the H atom detection laser beams (121.6 and 365 nm). Coherent light source at 121.6 nm was generated by difference FWM of two 212.6 nm photons and one 845 nm photon in a clean stainless steel cell filled with a 3:1 ratio Ar/Kr gas mixture. The mixing cell was sealed at both ends with a quartz window at

DOI:10.1063/1674-0068/cjcp2001008

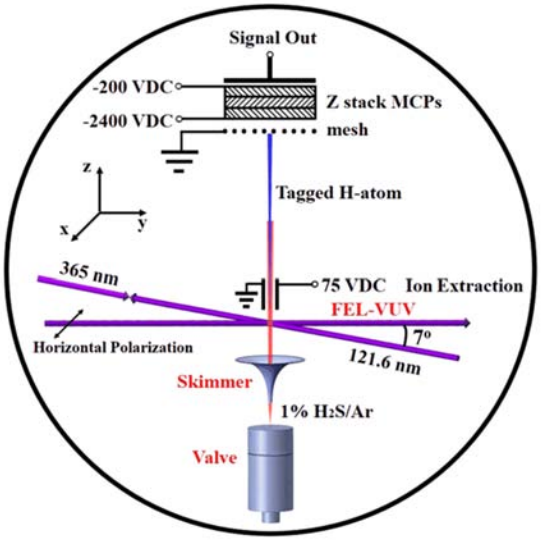

FIG. 1 The schematic view of photodissociation of H_2S by using the VUV FEL laser beam combined with the HRTOF technique.

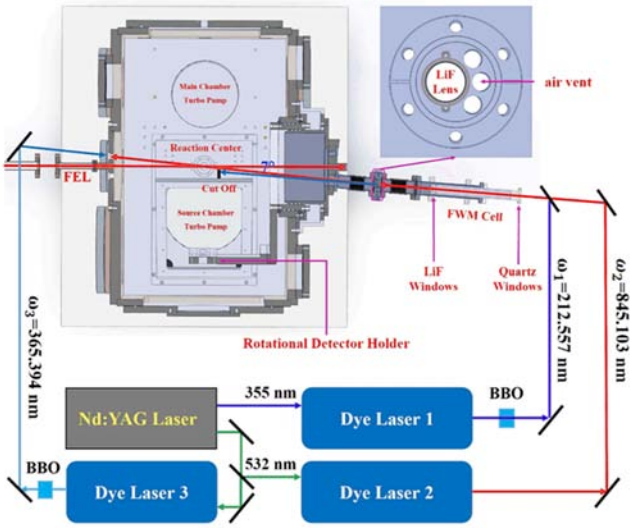

FIG. 2 The horizontal cutaway view of our experimental apparatus and the schematic view of the laser systems for the H atom detection.

the entrance and an LiF window at the light exit. Laser light at 212.6 nm was produced by doubling the output of a 355 nm (Nd:YAG laser, Spectra Physics Pro-290, 30 Hz) pumped dye laser (Sirah, PESC-G-24) operating at ∼425 nm. A half of the 532 nm output of the same Nd:YAG laser was used to pump another dye laser (Continuum ND6000) operated at ∼845 nm. These two beams were then focused into a cell by an achromatic lens (f=200 mm) to generate 121.6 nm using the difference FWM technique. To make sure the focus spots of these two beams spatially overlap, the 845 nm light was pre-focused by another lens (f=1500 mm). By adjusting the pressure of the mixing gas, the optimal VUV radiation at 121.6 nm was generated in the same direction with the fundamental beams of 212.6 nm and 845 nm. For some molecular systems, the 212.6 nm light will cause large background signals when it crosses the photodissociation region. Thus, the three beams then intersected an off-axis biconvex LiF lens (f=160 mm at 121.6 nm), where the VUV beam was dispersed from the UV beam. The biconvex lens was mounted on an aluminum flange, which allows the lens to slide off axis under vacuum conditions. By adjusting the position of the off-axis biconvex lens, the deflection angle and thus the direction of the VUV beam can be varied. The 365 nm laser light, exciting the H atom from the n=2 state to a high Rydberg state (n=30−80), was generated by doubling the output of a third dye laser (Radiant Dye Laser-Jaguar, D90MA) operating at ∼730 nm, pumped by the remaining of the 532 nm output of the Nd:YAG laser.

The VUV FEL laser was used as the photodissociation laser, which was operated at 10 Hz and the maximum pulse energy was ∼500 μJ/pulse (∼3×10^{14} photons/pulse) with the wavelength continuously tuning between 50−150 nm. This light had horizontal polarization and went into the main chamber through the vacuum tube, which was perpendicular to the front side of the chamber and connected the port on the chamber. To avoid the multi-photon dissociation, the pulsed energy of the FEL laser was suppressed as low as possible. In this experiment, we fixed the FEL laser energy to be about 5 μJ/pulse. The crossing angle of the detection laser beams ((121.6+365) nm) and the VUV FEL light beam was around 7°. The MCP detector was rotated in the plane that was perpendicular to the VUV FEL beam, so that the signal with the detection axis parallel (0°) and perpendicular (90°) to the photolysis laser polarization can be both recorded by rotating the MCP detector. A molecular beam of H_2S was generated by expanding a mixing of H_2S and Ar at a stagnation pressure of 600−900 torr through a 0.5 mm diameter pulsed nozzle (General Valve) and was perpendicular to the VUV FEL propagating direction. To record the signal from the VUV FEL photodissociation, we can subtract the 121.6 nm background signal by turning the VUV FEL beam on and off. In this experiment, the signal ratio of 122.95 nm to 121.6 nm is controlled to be about 50/1.

III. RESULTS AND DISCUSSION

Photodissociation of H_2S in the VUV region has long served as the prototype system for molecular photodissociation because of its important role in atmospheric chemistry and interstellar chemistry. Many experimental [28, 36–47] and theoretical [48–51] studies have been performed on this system during the last few decades. Similar to H_2O [52], the adsorption spectrum of H_2S [28]

DOI:10.1063/1674-0068/cjcp2001008

displays a series of peaks. The first absorption band of H_2S peaks at ∼195 nm with a progression of structures superimposed upon the broad continuum extending to ∼270 nm. Previous studies showed that photodissociation of H_2S in this band provided an ideal model of the direct dissociation, yielding an H atom and a ground state SH($X^2\Pi$) with little internal excitation [44–46]. As the excitation energy increased, the SH(X) product showed moderate vibrational excitation and cold rotational excitation.

From 160 nm to 118 nm, there are many strong absorption peaks which were assigned to several Rydberg series. In this region, only few studies were reported so far for the photodissociation of H_2S, which were conducted by Schnieder *et al.* [36] and Cook *et al.* [37] at 121.6 nm, and by Liu *et al.* [47] at 157.6 nm. The SH(X)+H channel was found to be the dominant dissociation process at 157.6 nm photolysis. The SH(X) products were both vibrationally and rotationally excited. An intriguing bimodal rotational distribution in the lowest two vibrational states (v=0 and 1) has been clearly observed, indicating that there are two distinctive dissociation mechanisms involved in the photodissociation of H_2S at 157.6 nm excitation. At 121.6 nm photolysis, however, the dissociation dynamics are much more complicated. Experimental studies revealed that the electronically excited SH($A^2\Sigma^+$) is predominant products, and no ground state SH(X) products are observed. The H atoms produced from the predissociation of SH(A) [53] can also be detected in the experiments, this makes it more difficult to determine the internal state distribution of the SH product and the branching ratios of the fragmentation pathways. Even though, the experimental results [36, 37] demonstrated that most of the SH(A) was in its vibrational ground state, with the rotational state distribution spanning almost all energetically available states (with the rotational level N up to over 40). High SH(A) vibrational states with v up to 4 were also considerably populated.

Since the light 212.6 nm can also photodissociate H_2S, none of the experimental studies have been performed in the H_2S photodissociation with the tunable VUV source generated by difference FWM technique. Actually, in the H_2S photodissociation at 157.6 nm, the background signal from 212.6 nm photolysis has already been observed and partially overlapped with that from 157.6 nm. The relative low intensity of the tunable VUV source (the power of VUV light is two orders of magnitude lower than that of 212.6 nm) prevent us from obtaining the signals from subtracting the background signal. FIG. 3 displays a comparision of the product translational energy distributions (E_T) from the photodissociation of H_2S at 121.6 nm with and without the light 212.6 nm in the photodissociation region (without and with the light dispersion method). It is obviously observed that the signal intensity from 212.6 nm photolysis is a few times stronger than that from 121.6 nm.

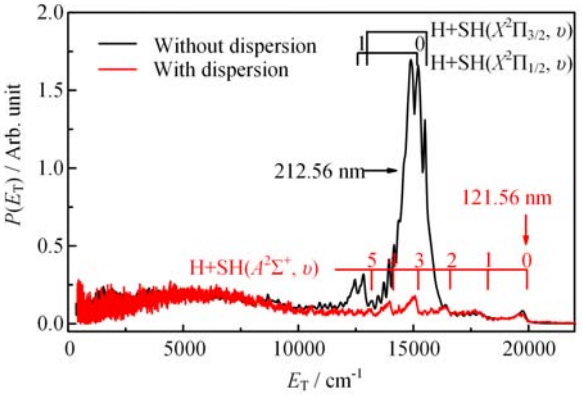

FIG. 3 The product translational energy distributions for H_2S photodissociation at 121.6 nm with the detection axis parallel to photolysis laser polarization. The black line was recorded without the laser dispersion and the red line was recorded with the laser dispersion.

The severe overlap prevents us extracting the signal from 121.6 nm photolysis. With the dispersion method, however, the signal from 212.6 nm photolysis totally disappears. We can easily get the results from the VUV photolysis with high signal to noise ratio. The results from the 121.6 nm photolysis of H_2S are similar to that reported in the literatures, suggesting our dispersion method works very well.

Using the above mentioned methods, we have studied photodissociation dynamics of H_2S at many wavelengths in the range 121.6−155 nm by using VUV FEL laser combined with the HRTOF technique. These results are reserved for a further study. Here we only show the result at 122.95 nm. The TOF profiles of H products have been recorded with the detection axis both parallel and perpendicular to the polarization vector of the photolysis laser. The derived total product translational energy spectra are exhibited in the FIG. 4. It is clear that a wealth of resolved structures associated with the various internal energy states of SH ($A^2\Sigma^+$) has been observed, which is similar to that at 121.6 nm [37]. At 122.95 nm photolysis, there are four energetically allowed H elimination fragmentation pathways for H_2S [36, 37]:

$$H_2S + h\nu \rightarrow H(^2S) + SH(X^2\Pi), \quad E_T \leq 49938 \text{ cm}^{-1}$$
$$H_2S + h\nu \rightarrow H(^2S) + SH(A^2\Sigma^+), \quad E_T \leq 18932 \text{ cm}^{-1}$$
$$H_2S + h\nu \rightarrow 2H(^2S) + S(^3P), \quad E_T \leq 19569 \text{ cm}^{-1}$$
$$H_2S + h\nu \rightarrow 2H(^2S) + S(^1D), \quad E_T \leq 10226 \text{ cm}^{-1}$$

The threshold energies for each pathway are marked by arrows in the FIG. 4. The E_T spectrum in the region of 20000 cm^{-1}−50000 cm^{-1} corresponds to the dissociation channel H+SH(X). A small intensity in this region suggests this channel is quite minor at 122.95 nm photolysis. The well-resolved structures below 20000 cm^{-1} can be assigned to the ro-vibrational states of SH(A) products. The combs in FIG. 4 show that the SH(A)

DOI:10.1063/1674-0068/cjcp2001008

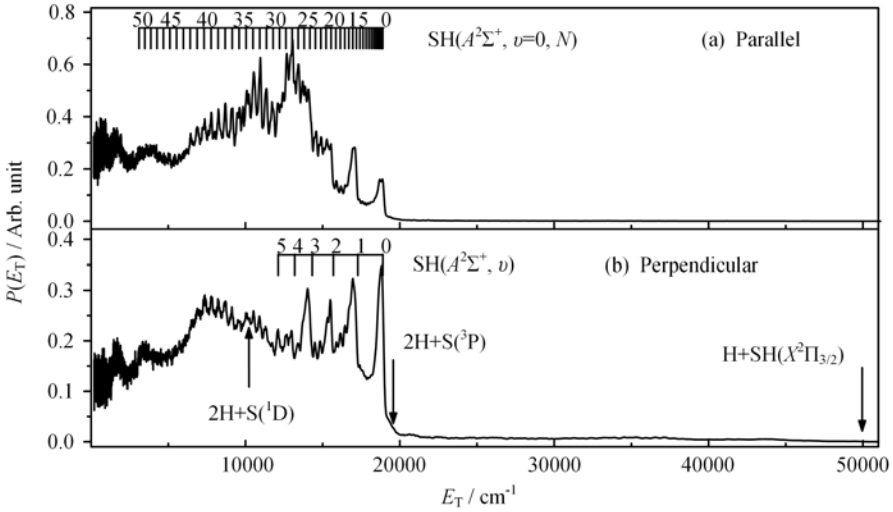

FIG. 4 The product translational energy distributions for H_2S photodissociation at 122.95 nm with the detection axis parallel (a) and perpendicular (b) to the VUV FEL laser polarization. All of the energetically allowed H elimination channels are marked by arrows.

fragments are formed mostly in low v levels but have rotational state distributions that extend to the highest N levels supported by the SH(A) potential energy function. The underlying broad peaks at low E_T may come from the three-body channels. The threshold energies for three-body channels S(^{1}D)+2H and S(^{3}P)+2H have been marked by downward pointing arrows.

According to the previous theoretical calculations [36], the topology of the $^1A_1$ ($\tilde{B}^1A_1$) surface of H_2S, which correlates adiabatically with the SH(A)+H asymptote, is markedly more complex than its H_2O counterpart. Along the S−H bond direction with little change of bond angle, the direct dissociation on $\tilde{B}^1A_1$ potential energy surface (PES) leads to the slightly vibrational SH($A^2\Sigma^+$) products (v=0−3). With great change of bond angle, one part of H_2S molecules will dissociate on the $\tilde{B}^1A_1$ PES producing extremely rotational SH($A^2\Sigma^+$) products, while another part will cross to the ground state PES by conical intersection (CI) and dissociate on the ground state producing the H(^{2}S)+SH($X^2\Pi$) products. However, based on the experimental results, the probability of dissociation through CI is quite small, indicating that the two CIs between $\tilde{B}^1A_1$ and X^1A_1 state is not important for dissociation dynamics of H_2S. The H−S−H bond angle in ground state H_2S is ∼92°, smaller than that for H_2O (∼104°), and a deep well appears in the Franck-Condon region of the $\tilde{B}$ state PES, all of these cause H_2S molecules to be hard to dissociate from the $\tilde{X}$ state PES through the CIs. In addition, the associated centrifugal forces could result in three body dissociation to H+H+S(^{1}D) products before the molecule had a chance to reach the linear configurations where nonadiabatic coupling to the lower surfaces (which correlate with H+SH(X) products) becomes effective. The detailed dissociation mechanism of H_2S still awaits further theoretical and experimental investigation. This experimental result suggests our setup is likely applicable to the tunable VUV photochemistry of many molecules that has significant H atom dissociation channels.

IV. CONCLUSION

A new experimental setup has been demonstrated for studying photochemistry using the high resolution time-of-flight Rydberg tagging technique, based on a laser dispersion method. By comparing the signal recorded with and without the laser dispersion, it is revealed that the laser dispersion is of great necessity for the study of H_2S photodissociation. Combining with the broadly tunable VUV FEL radiation source, photodissociation of H_2S was studied at 122.95 nm. Experimental results showed that the background signal from 212.6 nm has been eliminated, and the VUV photodissociation with high signal to noise ratio is clearly feasible. This technique is also likely applicable to the photochemistry of many other molecular systems (such as NH_3, CH_4, C_2H_6, *etc.*) in the VUV region that is important in the atmospheric and interstellar chemistry.

V. ACKNOWLEDGMENTS

This work was supported by the Strategic Priority Research Program of the Chinese Academy of Sciences (No.XDB17000000), the National Natural Science Foundation of China (NSFC Center for Chemical Dynamics (No.21688102)), the National Natural Science Foundation of China (No.21673232, No.21873099, No.21922306), and the International Partnership Program of Chinese Academy of Sci-

DOI:10.1063/1674-0068/cjcp2001008

ences (No.121421KYSB20170012). Li Che is supported by the National Natural Science Foundation of China (No.21973010). Zhi-chao Chen is supported by the National Natural Science Foundation of China (No.21773236). Zhi-guo Zhang is supported by the Natural Science Research Project of Education Department of Anhui Province (No.KJ2019A0521).

[1] E. F. van Dishoeck, E. Herbst, and D. A. Neufeld, Chem. Rev. **113**, 9043 (2013).
[2] K. J. Yuan, R. N. Dixon, and X. M. Yang, Acc. Chem. Res. **44**, 369 (2011).
[3] G. H. C. New and J. F. Ward, Phys. Rev. Lett. **19**, 556 (1967).
[4] R. Mahon, T. J. McIlrath, and D. W. Koopman, Appl. Phys. Lett. **33**, 305 (1978).
[5] R. Mahon and Y. M. Yiu, Opt. Lett. **5**, 279 (1980).
[6] R. Hilbig and R. Wallenstein, Appl. Opt. **21**, 913 (1982).
[7] K. Yuan, L. Cheng, Y. Cheng, Q. Guo, D. Dai, and X. Yang, Rev. Sci. Instrum. **79**, 124101 (2008).
[8] Y. Chang, S. Yu, Q. Li, Y. Yu, H. Wang, S. Su, Z. Chen, L. Che, X. Wang, W. Zhang, D. Dai, G. Wu, K. Yuan, and X. Yang, Rev. Sci. Instrum. **89**, 063113 (2018).
[9] J. J. Lin, J. Zhou, W. Shiu, and K. Liu, Rev. Sci. Instrum. **74**, 2495 (2003).
[10] D. H. Parker and A. T. J. B. Eppink, J. Chem. Phys. **107**, 2357 (1997).
[11] N. Saito, Y. Oishi, K. Miyazaki, K. Okamura, J. Nakamura, O. A. Louchev, M. Iwasaki, and S. Wada, Opt. Express. **24**, 7566 (2016).
[12] L. P. Shi, W. X. Li, H. Zhou, D. Wang, L. E. Ding, and H. P. Zeng, Phys. Rev. A **88**, 053825 (2013).
[13] W. Cao, E. R. Warrick, A. Fidler, S. R. Leone, and D. M. Neumark, Phys. Rev. A **94**, 021802 (2016).
[14] D. Normand, J. Morellec, and J. Reif, J. Phys. B: At. Mol. Opt. Phys. **16**, L227 (1983).
[15] K. S. E. Eikema, J. Walz, and T. W. Hänsch, Phys. Rev. Lett. **83**, 3828 (1999).
[16] D. R. Albert, D. L. Proctor, and H. F. Davis, Rev. Sci. Instrum. **84**, 063104 (2013).
[17] J. P. Marangos, N. Shen, H. Ma, M. H. R. Hutchinson, and J. P. Connerade, J. Opt. Soc. Am. B **7**, 1254 (1990).
[18] G. Hilber, A. Lago, and R. Wallenstein, J. Opt. Soc. Am. B **4**, 1753 (1987).
[19] B. Jones, J. Zhou, L. Yang, and C. Y. Ng, Rev. Sci. Instrum. **79**, 123106 (2008).
[20] X. Yang, J. Lin, Y. T. Lee, D. A. Blank, A. G. Suits, and A. M. Wodtke, Rev. Sci. Instrum. **68**, 3317 (1997).
[21] H. Wang, Y. Yu, Y. Chang, S. Su, S. Yu, Q. Li, K. Tao, H. Ding, J. Yang, G. Wang, L. Che, Z. He, Z. Chen, X. Wang, W. Zhang, D. Dai, G. Wu, K. Yuan, and X. Yang, J. Chem. Phys. **148**, 124301 (2018).
[22] Y. Chang, Y. Yu, H. Wang, X. Hu, Q. Li, J. Yang, S. Su, Z. He, Z. Chen, L. Che, X. Wang, W. Zhang, G. Wu, D. Xie, M. N. R. Ashfold, K. Yuan, and X. Yang, Nat. Commun. **10**, 1250 (2019).
[23] K. Yuan, Y. Cheng, L. Cheng, Q. Guo, D. Dai, X. Wang, X. Yang, and R. N. Dixon, Proc. Natl. Acad. Sci. USA **105**, 19148 (2008).
[24] S. A. Harich, D. W. H. Hwang, X. Yang, J. J. Lin, X. Yang, and R. N. Dixon, J. Chem. Phys. **113**, 10073 (2000).
[25] R. N. Dixon, D. W. Hwang, X. F. Yang, S. Harich, J. J. Lin, and X. Yang, Science **285**, 1249 (1999).
[26] C. Xiao, X. Xu, S. Liu, T. Wang, W. Dong, T. Yang, Z. Sun, D. Dai, X. Xu, D. H. Zhang, and X. Yang, Science **333**, 440 (2011).
[27] T. Yang, J. Chen, L. Huang, T. Wang, C. Xiao, Z. Sun, D. Dai, X. Yang, and D. H. Zhang, Science **347**, 60 (2015).
[28] L. C. Lee, X. Wang, and M. Suto, J. Chem. Phys. **86**, 4353 (1987).
[29] Y. J. Wu, H. C. Lu, H. K. Chen, B. M. Cheng, Y. P. Lee, and L. C. Lee, J. Chem. Phys. **127**, 154311 (2007).
[30] P. Saraswathy, K. Sunanda, S. Aparna, and B. N. Raja Sekhar, Spectro. Lett. **43**, 290 (2010).
[31] F. Z. Chen and C. Y. R. Wu, J. Quant. Spectrosc. RA **85**, 195 (2004).
[32] G. R. Wu, B. Jiang, Q. Ran, J. Zhang, S. A. Harich, and X. Yang, J. Chem. Phys. **120**, 2193 (2004).
[33] G. R. Wu, J. H. Zhang, S. A. Harich, and X. M. Yang, Chin. J. Chem. Phys. **19**, 109 (2006).
[34] J. Zhou, B. Jones, X. Yang, W. M. Jackson, and C. Y. Ng, J. Chem. Phys. **128**, 014305 (2008).
[35] S. J. Hanna, P. Campuzano-Jost, E. A. Simpson, D. B. Robb, I. Burak, M. W. Blades, J. W. Hepburn, and A. K. Bertram, Int. J. Mass Spectrom. **279**, 134 (2009).
[36] L. Schnieder, W. Meier, K. H. Welge, M. N. R. Ashfold, and C. M. Western, J. Chem. Phys. **92**, 7027 (1990).
[37] P. A. Cook, S. R. Langford, R. N. Dixon, and M. N. R. Ashfold, J. Chem. Phys. **114**, 1672 (2001).
[38] J. Delwiche and P. Natalis, Chem. Phys. Lett. **5**, 564 (1970).
[39] W. G. Hawkins and P. L. Houston, J. Chem. Phys. **73**, 297 (1980).
[40] W. G. Hawkins, J. Chem. Phys. **76**, 729 (1982).
[41] Z. Xu, B. Koplitz, and C. Wittig, J. Chem. Phys. **87**, 1062 (1987).
[42] J. Steadmana and T. Baer, J. Chem. Phys. **91**, 6113 (1989).
[43] B. R. Weiner, H. B. Levene, J. J. Valentini, and A. P. Baronavski, J. Chem. Phys. **90**, 1403 (1989).
[44] X. Xie, L. Schnieder, H. Wallmeier, R. Boettner, K. H. Welge, and M. N. R. Ashfold, J. Chem. Phys. **92**, 1608 (1990).
[45] R. E. Continetti, B. A. Balko, and Y. T. Lee, Chem. Phys. Lett. **182**, 400 (1991).
[46] S. H. S. Wilson, Mol. Phys. **88**, 841 (1996).
[47] X. Liu, D. W. Hwang, X. F. Yang, S. Harich, J. J. Lin, and X. Yang, J. Chem. Phys. **111**, 3940 (1999).
[48] R. N. Dixon, C. C. Marston, and G. G. Balint-Kurti, J. Chem. Phys. **93**, 6520 (1990).
[49] K. Weide, V. Staemmler, and R. Schinke, J. Chem. Phys. **93**, 861 (1990).
[50] B. Heumann, K. Weide, R. Düren, and R. Schinke, J. Chem. Phys. **98**, 5508 (1993).
[51] D. Simah, B. Hartke, and H. J. Werner, J. Chem. Phys. **111**, 4523 (1999).
[52] L. C. Lee and M. Suto, Chem. Phys. **110**, 161 (1986).
[53] S. M. Resende and F. R. Ornellas, J. Chem. Phys. **115**, 2178 (2001).

DOI:10.1063/1674-0068/cjcp2001008